

IMECE2002-34293

DEVELOPMENT OF MEMS MICROCHANNEL HEAT SINKS FOR MICRO/NANO SPACECRAFT THERMAL CONTROL

Anthony D. Paris
Jet Propulsion Laboratory
4800 Oak Grove Dr M/S 125-109
Pasadena, CA 91109-8099
Ph:818-393-6732 Fax:818-393-1633
Anthony.D.Paris@jpl.nasa.gov

Gajanana C. Birur
Jet Propulsion Laboratory
4800 Oak Grove Dr M/S 125-109
Pasadena, CA 91109-8099
Ph:818-354-4762 Fax:818-393-1633
gaj.birur@jpl.nasa.gov

Amanda A. Green
Jet Propulsion Laboratory
4800 Oak Grove Dr M/S 302-306
Pasadena, CA 91109-8099
Ph:818-393-2328 Fax:818-393-6047
Amanda.A.Green@jpl.nasa.gov

ABSTRACT

MEMS-based microchannel heat sinks are being investigated at the Jet Propulsion Laboratory (JPL) for use in micro/nano spacecraft thermal control. The current stage of development focuses on the integration of microchannel heat sinks into spacecraft pumped cooling loops. Two microchannel heat sinks, adapted from a Stanford University Microfluidics Laboratory design, were fabricated at JPL and tested for thermal and hydraulic performance in a single-phase pumped cooling loop. The first microchannel heat sink design was demonstrated to remove heat fluxes of up to 25 W/cm^2 with a maximum device temperature of less than $80 \text{ }^\circ\text{C}$. Both first and second generation heat sinks were shown to meet hydraulic performance criteria requiring less than 1 psi pressure drop with water as the working fluid. It was concluded that the design methodology developed for this project produces microchannel heat sink devices capable of high heat flux removal in future micro/nano spacecraft thermal control architecture.

INTRODUCTION

Future spacecraft designed for deep space science exploration are expected to be orders of magnitude smaller and lighter than those used today. Presently, the mass of such spacecraft range from 500 to 2000 kg. The National Aeronautics and Space Administration (NASA), through its

New Millennium Program, seeks to reduce the mass of these spacecraft by an order of magnitude in the next decade and by two orders of magnitude in the longer term [1]. Conceptual spacecraft that meet these mass specifications are referred to as micro- or nano- spacecraft. Despite the mass savings, these microspacecraft are expected to meet or exceed the current functionality of conventional spacecraft. Thus, the desired mass reduction must be achieved by miniaturization of individual components or integration of several components into smaller mass/volume packages. Unfortunately, these same processes increase the difficulty and complexity of spacecraft thermal control.

Microspacecraft thermal control design is more challenging than traditional, larger spacecraft thermal control design for several reasons. First of all, power requirements for microspacecraft are not expected to drop commensurately with their reduction in size. Although anticipated power levels range from a modest 10 to 50 W, the resultant power densities of the electronics, instrumentation, and avionics in microspacecraft may exceed those of traditional spacecraft by an order of magnitude or more. Secondly, the large reduction in spacecraft mass also reduces the overall heat capacity of the system. Since the primary power dissipation mode on these spacecraft may last only a small fraction of the mission time, the thermal control design is charged with not only high heat flux removal, but also energy conservation and component

temperature control. Thirdly, mission objectives for microspacecraft are likely to require exposure to more extreme thermal environments than have been encountered in the past. Smaller spacecraft are ideal for lander and sample return missions and may be required to survive harsh planetary thermal environments.

Solutions to the microspacecraft thermal control problem will require advanced thermal control technologies and architectures. Some thermal technologies requiring development are: high heat flux removal apparatus, light weight thermal insulation, deployable smart radiators, thermal storage phase change materials, and pumped cooling loops. An advanced thermal control architecture (Fig. 1) incorporating these technologies is currently being investigated at the Thermal and Propulsion Engineering section of JPL [2]. This architecture is an outgrowth of the Heat Rejection System (HRS) developed for the Mars Pathfinder mission in the mid-1990s [3]. The foundation of this thermal control system is a liquid pumped cooling loop capable of transporting large amounts of heat between spacecraft components and/or radiators.

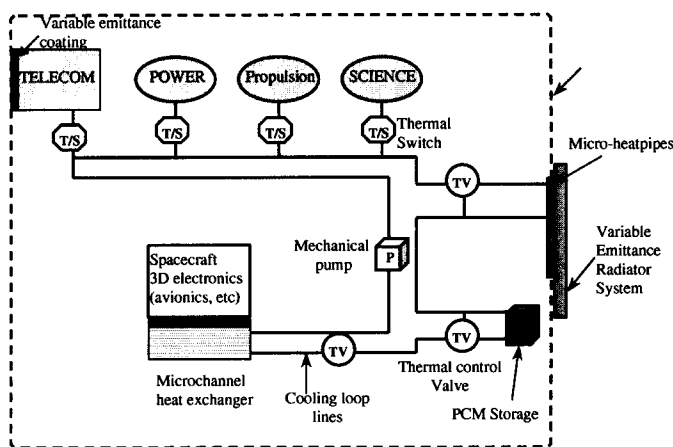


Figure 1. Advanced thermal control architecture

High heat flux removal technology is perhaps the most critical component of effective microspacecraft thermal control. A number of high heat flux cooling schemes including pool and channel flow boiling, spray and jet impingement flows, and microchannel heat sinks have been heavily researched over the past several years [4]. Of these cooling schemes, microchannel heat sinks are the most compatible with the thermal control architecture shown in Fig. 1. Microchannel heat sinks may be bonded directly onto the high power density electronic components of the microspacecraft and then integrated into the existing pumped cooling loop. The compact size of the microchannel heat sink would contribute little additional mass to the thermal control subsystem.

The study of high heat flux microchannel heat exchangers has been ongoing for the past two decades. Essentially, these devices are capable of high heat flux cooling because enormous single-phase heat transfer coefficients are associated with laminar forced convection when the hydraulic diameter of flow channels are greatly reduced. Tuckerman and Pease [5,6] first

demonstrated this principle by fabricating microchannel heat sinks capable of cooling upwards of 1000 W/cm^2 . A number of other researchers have subsequently investigated both single-phase and two-phase cooling in microchannel heat sinks with even more impressive results. Although beyond the scope of this paper, a thorough review of the theory and development of microchannel heat sinks may be found in "The MEMS Handbook" [7].

The objective of the present work is to design and test microchannel heat sinks compatible with microspacecraft thermal control applications. This goal entails not only meeting thermal and hydraulic performance criteria, but also accounting for component reliability and integration concerns.

NOMENCLATURE

q	power (W)
h	heat transfer coefficient ($\text{W/m}^2 \text{ K}$)
T	temperature ($^{\circ}\text{C}$)
R	thermal resistance ($^{\circ}\text{C/W}$)
m	mass flow rate (kg/s)
C_p	coolant specific heat (kJ/kg K)
HRS	Heat Rejection System
JPL	Jet Propulsion Laboratory
MDL	Microdevices Laboratory
RTD	Resistance Temperature Detector

HEAT SINK DESIGN REQUIREMENTS

The microchannel heat sinks tested in this study were designed to meet thermal requirements based on expected heat loads in microspacecraft. Typical high power-density units on current spacecraft include avionics (on-board processors, power processors, Inertial Management Units), telecom (solid state power amplifier, deep space transponder, UHF transmitter), and science payload. To reduce the power density of these units, the mechanical housing of their electronics are designed in such a way as to increase their footprint and thermal mass. As a result, the power density of current electronics modules on spacecraft is low (1 to 5 W/cm^2). However, excessive thermal masses are expected to be eliminated in future microspacecraft, and the resultant power densities in these units may grow to be as large as 25 W/cm^2 . As a result, 25 W/cm^2 is an appropriate benchmark for microspacecraft thermal technology development. Additionally, since allowable flight temperatures for spacecraft electronic components rarely exceed $80 \text{ }^{\circ}\text{C}$, high heat fluxes must be removed from the components at relatively low temperatures.

Single-phase cooling is the preferred mode of operation for our microchannel heat sinks due to the modest cooling requirement of 25 W/cm^2 . Additionally, there are a number of key reasons why single-phase coolants are preferred for spacecraft pumped cooling loops. These include: 1) extensive heritage of single-phase loop usage on aerospace applications, 2) simplicity and flexibility of cooling loop design, 3) increased pump reliability, and 4) insensitivity of cooling capacity to gravitational effects. However, in general, single-phase cooling requires a larger flow rate than two-phase cooling, and the magnitude of the pressure drop across a microchannel heat sink

is a concern at higher flow rates. Mechanically pumped cooling technology developed for Mars Pathfinder [3] used centrifugal pumps with hydrodynamic bearings to circulate a single-phase fluid in the spacecraft heat rejection system. Although centrifugal pumps are suitable for the long operation times associated with spacecraft missions, the pressure head produced by these pumps is generally small, typically 6 to 8 psi (40-50 kPa). This small pressure rise capacity of the pumps requires that the heat exchangers of the cooling system be designed such that they have a small pressure drop at the required flow rate (usually 1-2 psi or 7-14 kPa).

The design requirements for the microchannel heat sinks in this study are based on thermal and hydraulic criteria outlined in the paragraphs above. The devices are to cool 25 W/cm^2 while maintaining maximum temperatures below $80 \text{ }^\circ\text{C}$. To insure compatibility with HRS pumped cooling loops, the pressure drop across the heat sinks should be no more than 2 psi at the designed flow rate.

MICROCHANNEL DEVICE DESIGN

Since microchannel heat sinks for terrestrial applications have been well investigated, it was decided that our study should be based upon a proven methodology. To that end, JPL granted a contract to Professor Tom Kenny at Stanford University for access to designs and materials developed at the Stanford University Microfluidics Laboratory for the study of microchannel heat sink devices. Researchers from this lab developed a MEMS-based parallel flow microchannel heat exchanger with implanted resistance heaters and thermistors to investigate primarily two-phase cooling. Design details for the devices and results from these studies may be found in a number of recent papers published by this research group [8-10]. The basic design of the Stanford microcooler device consists of a number of parallel, rectangular microchannels positioned between two fluid manifolds. The channel and manifold regions are etched from a silicon wafer that is subsequently capped with a layer of Pyrex glass. Inlet and outlet holes etched into the wafer allow fluid to enter the inlet manifold, flow through the channels, collect in the outlet manifold, and exit the microcooler. Heating and temperature sensing elements are implanted into the silicon wafer beneath the microchannels and electrical connections are made from these elements to an attached surfboard. A ZIF socket mated with the surfboard allows connections with power supplies and sensing electronics.

The microchannel heat sinks of our study are based on this Stanford design. The footprint of the microchannels (3.5 cm^2) is typical of microspacecraft electronic components and the integrated heaters can apply high heat fluxes. However, due to our different applications and the fabrication capabilities at JPL, a number of changes have been made to this basic design. To meet our single-phase cooling performance criteria, the microchannel dimensions were re-designed. A numerical model based on MICROHEX, a FORTRAN code developed by Phillips [11], was used to determine the optimal channel geometry. The major assumptions in the model are: steady and incompressible coolant flow, spatially and temporally constant power dissipation, isotropic thermal conductivity, uniform fin

thickness, adiabatic cover plate, negligible radiation and convection heat transfer, uniform fin-base temperature, identical fin-base and channel-base temperature, and uniform coolant temperature and heat transfer coefficient at a given axial distance [12]. Using a simple energy balance for the fluid, $q = mc_p(T_{out} - T_{in})$, the mass flow rate of the coolant must be 20 ml/min if the fluid is water, the footprint of the microchannel heat exchanger is 3.5 cm^2 , and the temperature difference is $65 \text{ }^\circ\text{C}$. To minimize the pressure drop, the microchannels are etched as deep as possible while leaving enough substrate at the channel base to prevent device cracking or leaking. For all model computations, the channel depth and length were maintained at 400 microns and 20 mm, respectively, while the microchannel spacing was set equal to the microchannel width. The variation of pressure drop and overall thermal resistance with microchannel width is presented in Fig. 2. For this plot, the thermal resistance is equal to the difference between the maximum chip temperature and the inlet coolant temperature divided by the total heat extracted. Although the pressure drop increases dramatically as the channel width is decreased from approximately 150 microns, the total thermal resistance varies by less than 10%. Based on this model, our heat sink microchannels were designed to be 150 microns wide, 400 microns deep, 20 mm long, and spaced 150 microns apart.

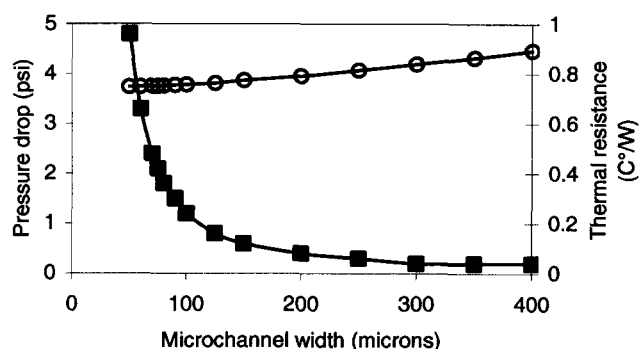


Figure 2. Microchannel width optimization (■ pressure drop, ○ thermal resistance)

Figure 3 shows a photograph of our first complete microchannel heat sink. The overall dimensions of the device are approximately 65 mm by 20 mm by 1 mm. The inlet and outlet holes are spaced 40 mm apart and connected by symmetric 3 mm by 7.5 mm neck regions, 17.8 mm by 3 mm rectangular manifolds, and a bank of 59 parallel microchannels. The neck and manifold dimensions are essentially the same as the Stanford design. These devices were fabricated in the Microdevices Lab (MDL) at JPL by duplicating the process for channel patterning and etching developed at Stanford [8]. The devices were fabricated in 500 micron thick polished silicon wafers. The manifolds and channels were patterned on the front side of the wafer and etched to a depth of 400 microns. Following this step, inlet and outlet holes were patterned and etched through on the backside of the wafer. Full wafer anodic bonding of a 500 micron thick Pyrex cover plate was used to seal the channels and allow for visual characterization of the flow. Dicing of the wafer released the individual devices (three per wafer) and a ten pin single-in-line surfboard was epoxied to the backside of each device.

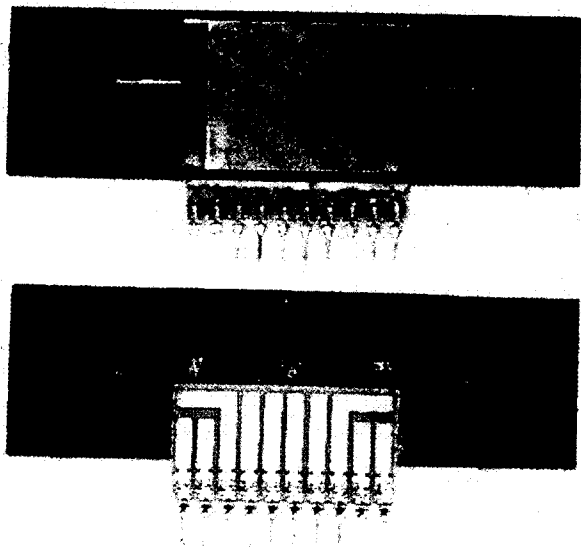


Figure 3. Photograph of the microchannel heat sink device; front (top) and back (bottom).

In order to facilitate complete device fabrication at MDL, the microchannel heat sink devices fabricated at JPL do not employ the same implanted resistors for heating and temperature sensing as the original Stanford design. Instead, a deposited metal film trace was chosen for the resistive heating element and encapsulated platinum RTDs were used to measure chip temperatures. The heater deposition occurred before the manifolds and channels were etched into the wafer. After a wet oxidation step, the heater trace was patterned as a serpentine trace 300 microns wide and 280 mm long that covered the 3.5 cm² footprint of the microchannels. Electron-beam evaporation was used to deposit titanium, platinum, and gold in layers on the wafer surface. The heater trace was revealed after a warm acetone soak and was 3200 Å thick with a nominal resistance of 140 Ohms at room temperature. The heater was connected to the surfboard via dual 25 micron gold wirebonds. Encapsulated platinum RTDs with a footprint of approximately 1.5 mm by 1 mm were procured from Hy-Cal Engineering. Three RTDs were affixed to the silicon surface by thermally conductive epoxy. They were positioned along the centerline of the device at locations corresponding to the channel inlet, mid-span, and outlet. Electrical connections from the RTD leads to the surfboard were made with 36 gauge wire and a combination of solder and electrically conductive epoxy. Nominal resistance of the RTDs at room temperature was 1090 Ohms. A photograph of the metal trace heater and RTD sensors can be seen in Figure 3.

TEST EQUIPMENT AND PROCEDURES

A facility was developed at JPL to test the performance of the microchannel heat sink devices within the context of a spacecraft heat rejection system. The test hardware consisted of a class 100 laminar flow bench, a mechanically pumped fluid cooling loop with microchannel test fixture, laboratory instrumentation, and a data acquisition system. All components of the cooling loop were rated for system pressures over 100

psig (0.7 MPa) and temperatures in the range of 100 to 200 °C. Although the loop was designed to test microchannel heat sink performance with a variety of liquid coolants, de-ionized water was used for all testing.

A diagram of the pumped cooling loop assembly is shown in Fig. 4. A Micropump series 180 magnetic drive gear pump provided continuous pressure head for circulating the coolant through the fluid loop with a maximum flow rate of approximately 70 ml/min. A Swagelok sample cylinder was positioned vertically and charged with gas to serve as a liquid accumulator. An inline rotameter was calibrated for water and measured flow rates up to 50 ml/min. Two Swagelok filters in series removed all micron-sized particles from the loop. A test fixture, fabricated from low thermal conductivity Utem material, allowed the microchannel heat sink devices to be connected to the stainless steel tubing used throughout the cooling loop assembly. Similar to the test hardware developed at the Stanford, this fixture used o-rings to create seals at the inlet and the outlet holes of the heat sink devices. Two macroscopic heat exchanger units were used to remove heat from the working fluid in the closed-loop assembly. The primary coil-in-shell heat exchanger was located after the test fixture and served to cool the working fluid to approximately 20 °C. A custom tube-in-shell design secondary heat exchanger was located just upstream of the test fixture and served to cool the working fluid below ambient laboratory temperature. A Neslab RTE-111 recirculating bath chiller was connected to both heat exchangers. The entire assembly (sans chiller) was situated on the laminar flow bench

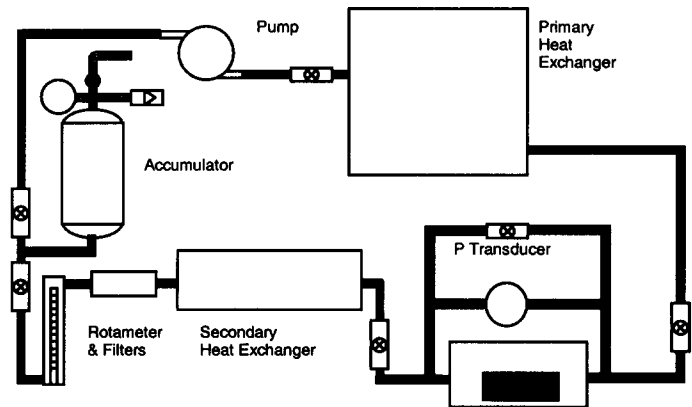


Figure 4. Pumped cooling loop test assembly

The pumped loop assembly was instrumented with a number of pressure and temperature sensors. Pressure gauges located before and after the Micropump and on the accumulator were used to monitor system pressure. A Validyne differential pressure transducer with a range of 0-2 psid (0-14 kPa) measured the pressure drop across the test fixture and microchannel device. Seven type E thermocouples measured tubing and test fixture surface temperatures. Three type E thermocouple probes were inserted into the working fluid at locations just upstream and downstream of the test fixture and downstream of the primary heat exchanger. An Agilent data logger was used to record measurements from the pressure transducer, thermocouples, and the heat sink RTDs. A Xantrex programmable DC power supply controlled the power applied

to the microchannel device heater. Both the data logger and power supply were configured and controlled over a GPIB interface with LabVIEW software.

RESULTS

The microchannel heat sink devices were tested for steady-state cooling performance. For a given flow rate and input heating power, the cooling loop was allowed to reach a state of thermal equilibrium as quantified by a temperature rise in the coolant of less than 2 °C/hr. Once reaching steady state, temperature and pressure data were collected at intervals of six seconds for approximately 30 minutes and then averaged. The coolant flow rate was monitored during this interval to insure a steady mass flow through the heat sink. Each test was performed at a loop system pressure of approximately 15 psig (200 kPa) with a coolant temperature of 21 °C at the inlet of the test fixture.

A test matrix comprised of flow rates from 10 to 25 ml/min and target cooling densities from 5 to 25 W/cm² was used to test the hydraulic and thermal performance of the microchannel heat sink devices. The voltage applied to the device heater was adjusted for each run so that the temperature rise in the coolant fluid across the test fixture would be equal to the desired cooling power divided by the product of the mass flow rate and coolant specific heat. This process allowed the data to be correlated based on heat flux into the microchannel heat sink device rather than total heater power consumption (which included parasitic heat losses from the test equipment.) Once the steady-state data was collected, the actual heat flux into the heat sink was determined from the net enthalpy change in the water and the mass flow rate.

Figure 5 shows the maximum chip temperature as measured by the platinum RTD located beneath the outlet manifold. From this plot, we can see that the silicon substrate was kept below the design limit of 80 °C for heat fluxes up to 23 W/cm². (A test with a heat flux greater than 25 W/cm² was not possible due to structural failure of the heat sink device.) Figure 6 also shows that higher chip temperatures are achieved at the same heat flux for lower flow rates, which is to be expected.

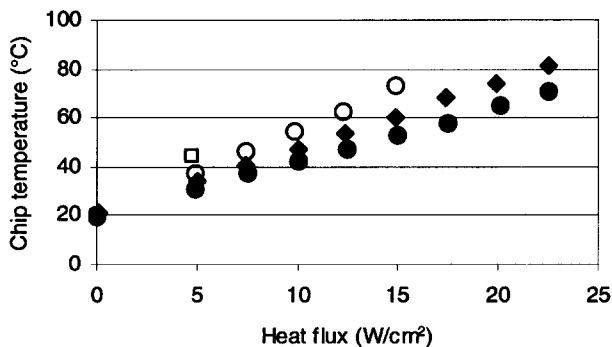


Figure. 5 Maximum chip temperature vs. heat flux for various coolant flow rates. Legend: ● 25 ml/min, ◆ 20 ml/min, ○ 15 ml/min, □ 10 ml/min.

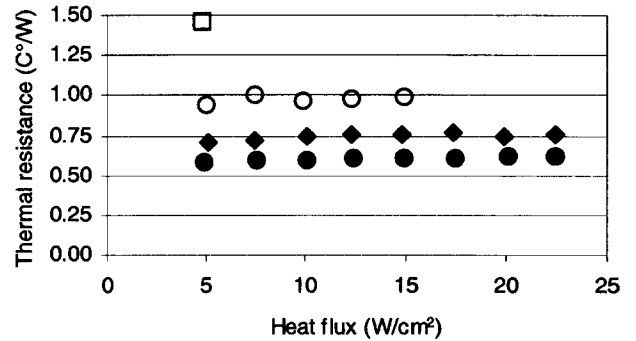


Figure. 6 Total thermal resistance vs. heat flux for various coolant flow rates. (see Fig. 5 for legend)

Figure 6 shows the variation of total thermal resistance of the heat sinks with heat flux and flow rate. Although there is little change in thermal resistance with heat flux, doubling the flow rate serves to approximately halve the resistance. This is largely due to the increased maximum chip temperature observed at the lower flow rates. Figure 7 shows the pressure drop across the devices for various flow rates and heat fluxes. It should be noted that the pressure drop through the test fixture is included in these data and serve to increase the pressure drop magnitude (albeit less than 10%). All pressure drops are below 0.5 psi (3.5 kPa)—well below the hydraulic performance design criterion of 2 psi. Additionally, there is a slight decrease in the pressure drop at the higher heat fluxes due to the decrease in the viscosity of the water as the temperature rises in the heat sink.

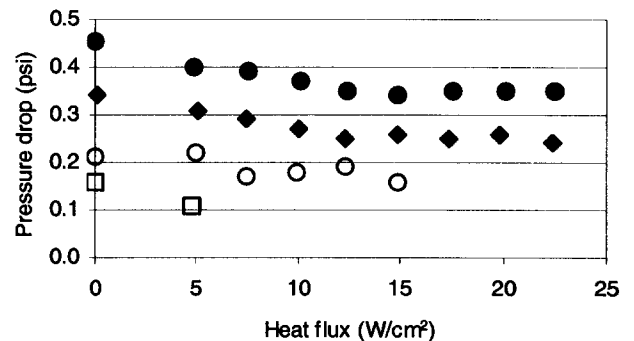


Figure.7 Microchannel heat sink pressure drop vs. heat flux at various coolant flow rates. (see Fig. 5 for legend)

REDESIGN EFFORTS

Although the microchannel heat sinks described in the previous sections met all design requirements, the devices were quite fragile and easily broken. The high failure rate of the devices prevented more extensive testing of the heat sinks with multiple coolant fluids. The two major failure modes in the devices were de-bonding of the Pyrex glass and silicon wafer in the microchannel area and structural failure of the silicon wafer in the manifold area. The heat sink devices were redesigned to

increase structural integrity while maintaining thermal and hydraulic performance.

Of the five heat sink devices fabricated, three failed by debonding of the Pyrex glass from the wafer. Since the debonding was found only in the microchannel area, it was surmised that there was insufficient surface area contact between the glass and the silicon wafer in this region. A redesign of the microchannel area decreased the width of the channel area from 17.8 mm to 13.3 mm and the length of the channels from 20 mm to 15 mm. By decreasing the width of the channel area, the bonding area to either side of the channels was increased three fold. However, this redesign also resulted in a reduction of microchannel footprint from 3.5 cm² to 2.0 cm².

Hydraulic testing of the microchannel heat sinks at elevated system pressures also revealed a failure mode associated with the manifold design. Due to the relatively large area of the manifold, the bending moment applied to the thin silicon wafer (100 microns) at the edges of the manifold was large enough at system pressures over 50 psig (500 kPa) to cause a fracture in the silicon. This failure mode, along with the fact that the original manifold design exacerbated pressure head losses due to flow separation, necessitated a redesign of the entrance and exit manifolds. A diffuser design with 100 micron wide intermediate flow vanes was chosen to decrease the exposed area of the manifold floor and reduce flow separation in the inlet manifold. Photographs of both manifold designs are shown in Fig. 8. To further strengthen the manifold area, the etching depth of the manifolds and microchannels was decreased so that the wafer thickness could be increased from 100 to 175 microns.

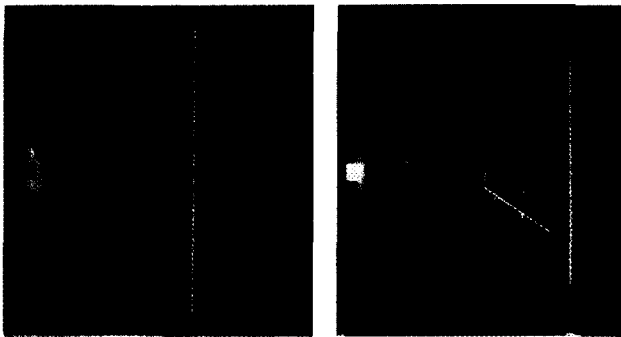


Figure 8. Microchannel manifold redesign; original manifold (left) and diffuser manifold (right)

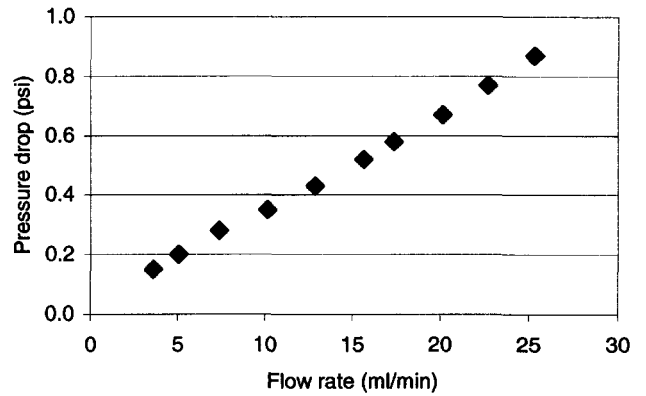


Figure 9. Hydraulic performance of the redesigned microchannel heat sink.

The decrease in channel depth from 400 to 325 microns necessitated a change in the channel width in order to meet the thermal and hydraulic performance requirements for the heat sink. Again, the numerical model was employed and an optimal channel width of 125 microns was chosen. The spacing between the channels was increased from 150 to 200 microns. The result was a set of 42 parallel channels, each 125 microns wide, 325 microns deep, and 15 mm long. For a flow rate of 25 ml/min of water and a heat flux of 25 W/cm², the numerical model predicted a total thermal resistance of 0.65 C°/W and pressure drop under 1 psi (7 kPa). Although thermal testing of the redesigned microchannel heat sinks was not completed at press time, pressure drop data (Fig. 9) indicate that the hydraulic performance meets the design goal of less than 1 psi.

CONCLUSIONS

MEMS-based microchannel heat sinks were investigated at the Jet Propulsion Laboratory (JPL) for use in micro/nano spacecraft thermal control. A parallel microchannel heat exchanger design by the Stanford University Microfluidics Laboratory was adapted to meet thermal and hydraulic performance requirements for microspacecraft thermal control. Microchannel heat sinks were fabricated at JPL and tested in a mechanically pumped fluid loop test assembly. Measurements included steady-state heat flux removal, maximum device temperatures, and pressure drop values. The first microcooler heat sink design was demonstrated to remove heat fluxes of up to 25 W/cm² while maintaining maximum device temperature of less than 80 C. Testing was conducted with water as the cooling fluid and pressure drops less than 1 psi were observed with flow rates up to 25 ml/min. A redesign of the heat sinks was conducted to increase structural integrity of the devices. The resultant design was shown to meet hydraulic design requirements. The results of this study indicate that the design methodology developed for this project produces microchannel heat exchanger devices capable of high heat flux removal in future micro/nano spacecraft thermal control. Future work on this project will involve the testing of microchannel heat sinks with various working fluids and the development of integrated

micropumps to allow the heat sinks to be decoupled from the heat rejection system coolant flow.

ACKNOWLEDGMENTS

The research described in this paper was conducted at the Jet Propulsion Laboratory, California Institute of Technology, under a contract with the National Aeronautics and Space Administration. The funds for the technology development were provided by the NASA 632 Cross Enterprise Technology Development Program (Dr. Elizabeth Kolawa, Program Manager, Micro/Nano Sciencecraft Technology Program at JPL.) The authors wish to thank Tricia Sur, Siina Haapanen, Judy Podosek, Lin Miller, and Steven Vargo for their important contributions to the early stages of this work. Professor Tom Kenny and the researchers at the Stanford University Microfluidics Laboratory are gratefully acknowledged for developing the basic design of the microchannel heat sink devices and for technical assistance with this project.

REFERENCES

- [1] Casani, E.K., 1996, "Reduced cost and increased capability through technology in the new millennium" *Acta Astronautica*, **39**(1-4), pp. 153-160.
- [2] Birur, G.C., and O'Donnell, T., 2001, "Advanced thermal control technologies for space science missions at Jet Propulsion Laboratory", *Proc. Space Technology Application International Forum*, M. El-Genk, ed., American Institute of Physics.
- [3] Birur G.C., and Bhandari, P., 1998, "Mars Pathfinder Active Heat Rejection System: Successful Flight Demonstration of a Mechanically Pumped Cooling Loop," SAE Technical Paper No. 981684, *28th International Conference on Environmental Systems*.
- [4] Mudawar, I., 2001, "Assessment of High-Heat-Flux Thermal Management Schemes", *IEEE Transactions On Components And Packaging Technologies*, **24**(2), pp. 122-141.
- [5] Tuckerman, D.B., and Pease, R.F.W., 1981, "High-performance Heat Sinking for VLSI," *IEEE Electron Device Letters*, EDL-2(5), pp. 126-129.
- [6] Tuckerman, D.B., 1984, "Heat-Transfer Microstructures for Integrated Circuits," Ph.D. thesis, Stanford University, Stanford, CA.
- [7] Gad-el-Hak, M., ed., 2002, *The MEMS Handbook*, CRC Press, Boca Raton, FL, Chap. 32.
- [8] Zhang, L., Banerjee, S.S., Koo, J., Laser, D.J., Asheghi, M., Goodson, K.E., Santiago, J.G., and Kenny, T.W., 2000, "A Micro Heat Exchanger with Integrated Heaters and Thermometers," *Proc. Solid State Sensor and Actuator Workshop*, pp. 275-280.
- [9] Zhang, L., Koo, J., Jiang, L., Goodson, K.E., Santiago, J.G., and Kenny, T.W., 2001, "Study of Boiling Regimes and Transient Signal Measurements in Microchannels," *Proc. Transducers'01*, **2**, pp. 1514-1517.
- [10] Zhang, L., Koo, J., Jiang, L., Asheghi, M., Goodson, K.E., Santiago, J.G., and Kenny, T.W., 2002, "Measurements and Modeling of Two-Phase Flow in Microchannels with Nearly Constant Heat Flux Boundary Conditions," *J. Microelectromechanical Systems*, **11**(1), pp. 12-19.
- [11] R. J. Phillips, "Forced-convection liquid-cooled microchannel heat sinks", Master's thesis, Massachusetts Institute of Technology, Cambridge, Massachusetts, 1987.
- [12] R. J. Phillips, "Microchannel Heat Sinks", in *Advances in thermal modeling of electronic components and systems*, A. Bar-Cohen, ed., vol. 2, pp. 109-184, Hemisphere Publishing Corp., New York, 1990.

is a concern at higher flow rates. Mechanically pumped cooling technology developed for Mars Pathfinder [3] used centrifugal pumps with hydrodynamic bearings to circulate a single-phase fluid in the spacecraft heat rejection system. Although centrifugal pumps are suitable for the long operation times associated with spacecraft missions, the pressure head produced by these pumps is generally small, typically 6 to 8 psi (40-50 kPa). This small pressure rise capacity of the pumps requires that the heat exchangers of the cooling system be designed such that they have a small pressure drop at the required flow rate (usually 1-2 psi or 7-14 kPa).

The design requirements for the microchannel heat sinks in this study are based on thermal and hydraulic criteria outlined in the paragraphs above. The devices are to cool 25 W/cm² while maintaining maximum temperatures below 80 °C. To insure compatibility with HRS pumped cooling loops, the pressure drop across the heat sinks should be no more than 2 psi at the designed flow rate.

MICROCHANNEL DEVICE DESIGN

Since microchannel heat sinks for terrestrial applications have been well investigated, it was decided that our study should be based upon a proven methodology. To that end, JPL granted a contract to Professor Tom Kenny at Stanford University for access to designs and materials developed at the Stanford University Microfluidics Laboratory for the study of microchannel heat sink devices. Researchers from this lab developed a MEMS-based parallel flow microchannel heat exchanger with implanted resistance heaters and thermistors to investigate primarily two-phase cooling. Design details for the devices and results from these studies may be found in a number of recent papers published by this research group [8-10]. The basic design of the Stanford microcooler device consists of a number of parallel, rectangular microchannels positioned between two fluid manifolds. The channel and manifold regions are etched from a silicon wafer that is subsequently capped with a layer of Pyrex glass. Inlet and outlet holes etched into the wafer allow fluid to enter the inlet manifold, flow through the channels, collect in the outlet manifold, and exit the microcooler. Heating and temperature sensing elements are implanted into the silicon wafer beneath the microchannels and electrical connections are made from these elements to an attached surfboard. A ZIF socket mated with the surfboard allows connections with power supplies and sensing electronics.

The microchannel heat sinks of our study are based on this Stanford design. The footprint of the microchannels (3.5 cm²) is typical of microspacecraft electronic components and the integrated heaters can apply high heat fluxes. However, due to our different applications and the fabrication capabilities at JPL, a number of changes have been made to this basic design. To meet our single-phase cooling performance criteria, the microchannel dimensions were re-designed. A numerical model based on MICROHEX, a FORTRAN code developed by Phillips [11], was used to determine the optimal channel geometry. The major assumptions in the model are: steady and incompressible coolant flow, spatially and temporally constant power dissipation, isotropic thermal conductivity, uniform fin

thickness, adiabatic cover plate, negligible radiation and convection heat transfer, uniform fin-base temperature, identical fin-base and channel-base temperature, and uniform coolant temperature and heat transfer coefficient at a given axial distance [12]. Using a simple energy balance for the fluid, $q = mc_p(T_{out}-T_{in})$, the mass flow rate of the coolant must be 20 ml/min if the fluid is water, the footprint of the microchannel heat exchanger is 3.5 cm², and the temperature difference is 65 °C. To minimize the pressure drop, the microchannels are etched as deep as possible while leaving enough substrate at the channel base to prevent device cracking or leaking. For all model computations, the channel depth and length were maintained at 400 microns and 20 mm, respectively, while the microchannel spacing was set equal to the microchannel width. The variation of pressure drop and overall thermal resistance with microchannel width is presented in Fig. 2. For this plot, the thermal resistance is equal to the difference between the maximum chip temperature and the inlet coolant temperature divided by the total heat extracted. Although the pressure drop increases dramatically as the channel width is decreased from approximately 150 microns, the total thermal resistance varies by less than 10%. Based on this model, our heat sink microchannels were designed to be 150 microns wide, 400 microns deep, 20 mm long, and spaced 150 microns apart.

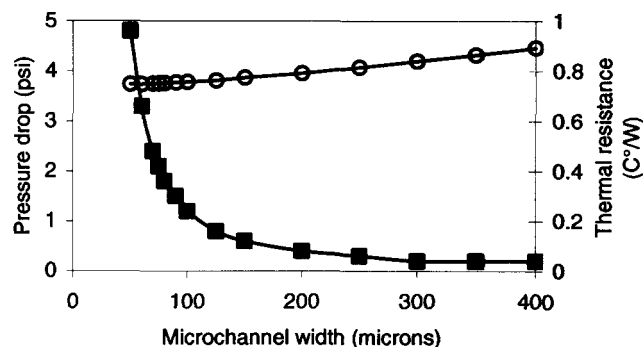


Figure 2. Microchannel width optimization (■ pressure drop, ○ thermal resistance)

Figure 3 shows a photograph our first complete microchannel heat sink. The overall dimensions of the device are approximately 65 mm by 20 mm by 1 mm. The inlet and the outlet holes are spaced 40 mm apart and connected by symmetric 3 mm by 7.5 mm neck regions, 17.8 mm by 3 mm rectangular manifolds, and a bank of 59 parallel microchannels. The neck and manifold dimensions are essentially the same as the Stanford design. These devices were fabricated in the Microdevices Lab (MDL) at JPL by duplicating the process for channel patterning and etching developed at Stanford. The devices were fabricated in four-inch (102 mm) diameter, 500 micron thick polished silicon wafers. The manifolds and channels were patterned on the front side of the wafer and deep reactive ion etching (DRIE) was used to etch them to a depth of 400 microns. Following this step, inlet and outlet holes were patterned and etched through on the backside of the wafer. Full wafer anodic bonding of a 500 micron thick Pyrex cover plate is used to seal the channels and allow for visual characterization of the flow. Dicing of the wafer releases the individual devices (three per wafer) and a ten pin single-in-line surfboard is epoxied to the backside of each device.

in the range from 100 to 200°C
over 100 psi

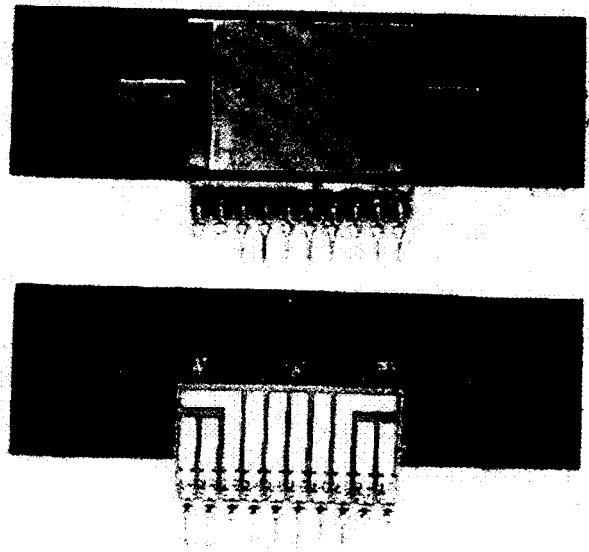


Figure 3. Photograph of the microchannel heat sink device; front (top) and back (bottom).

In order to facilitate complete device fabrication at MDL, the microchannel heat sink devices fabricated at JPL do not employ the same implanted resistors for heating and temperature sensing as the original Stanford design. Instead, a deposited metal film trace was chosen for the resistive heating element and encapsulated platinum RTDs were used to measure chip temperatures. The heater deposition occurred before the manifolds and channels were etched into the wafer. After a wet oxidation step at a temperature of 1050 °C produced an oxidation layer approximately 0.5 microns thick on the wafer, the heater trace was patterned. The heater was patterned as a serpentine trace 300 microns wide and 280 mm long that covers the 3.5 cm² footprint of the microchannels. Electron beam evaporation was used to deposit 300 Å titanium, 600 Å Platinum, and 2800 Å gold in layers on the wafer surface. The heater trace was revealed after a warm acetone soak and was 3200 Å thick with a nominal resistance of 140 Ohms at room temperature. The heater was connected to the surfboard via dual 25 micron gold wirebonds. Encapsulated platinum RTDs with a footprint of approximately 1.5 mm by 1 mm were procured from Hy-Cal Engineering. Three RTDs were affixed to the silicon surface by Omegabond 401 thermal epoxy. They were positioned along the centerline of the device at locations corresponding to the channel inlet, mid-span, and outlet. Electrical connections from the RTD leads to the surfboard were made with 36 gauge copper wire and a combination of solder and Epoxi-Bond epoxy. Nominal resistance of the RTDs at room temperature was 1090 Ohms. A photograph of the metal trace heater and RTD sensors can be seen in Figure 3.

TEST EQUIPMENT AND PROCEDURES

A facility was developed at JPL to test the performance of the microchannel heat sink devices within the context of a spacecraft heat rejection system. The test hardware consisted of a class 100 laminar flow bench, a mechanically pumped fluid cooling loop with microchannel test fixture, laboratory

instrumentation, and a data acquisition system. All components of the cooling loop were rated for system pressures up to 200 psig (1.5 MPa) and temperatures up to 200 °C. Although the loop was designed to test microchannel heat sink performance with a variety of liquid coolants, de-ionized water was used for all testing.

A diagram of the pumped cooling loop assembly is shown in Fig. 4. A Micropump series 180 magnetic drive gear pump provided continuous pressure head (75 psi max) for circulating the coolant through the fluid loop with a maximum flow rate of approximately 70 ml/min. A 150 ml Swagelok sample cylinder was positioned vertically and charged with nitrogen gas to serve as a liquid accumulator. An inline rotameter was calibrated for water and measured flow rates up to 50 ml/min with a resolution of 0.2 ml/min. Two Swagelok filters in series removed particles larger than 7 and 0.5 microns. A test fixture, fabricated from low thermal conductivity Ultem material, allowed the microchannel heat sink devices to be connected to the 1/8" stainless steel tubing used throughout the cooling loop assembly. Similar to the test hardware developed at the Stanford, this fixture used o-rings to create seals at the inlet and the outlet holes of the heat sink devices. Two macroscopic heat exchanger units were used to remove heat from the working fluid in the closed-loop assembly. The primary heat exchanger (Stanford Equipment Corp sample cooler) was located after the test fixture and served to cool the working fluid to approximately 20 °C. A custom tube-in-shell design secondary heat exchanger was located just upstream of the test fixture and served to cool the working fluid below ambient laboratory temperature. A Neslab RTE-111 recirculating bath chiller was connected to both heat exchangers and was capable of extracting up to 500 W of heat. The entire assembly (sans chiller) was situated on the laminar flow bench

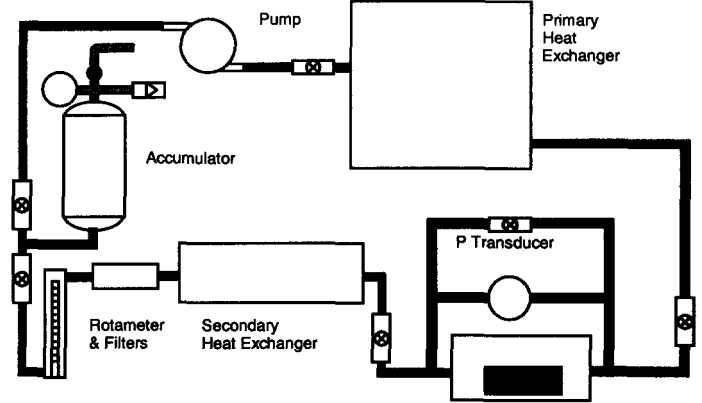


Figure 4. Pumped cooling loop test assembly

The pumped loop assembly was instrumented with a number of pressure and temperature sensors. Pressure gauges located before and after the Micropump and on the accumulator were used to monitor system pressure. A Validyne differential pressure transducer with a range of 0-2 psid (0-14 kPa) measured the pressure drop across the test fixture and microchannel device. Seven type E thermocouples measured the pressure tubing and test fixture surface temperatures. Three type E thermocouple probes were inserted into the working fluid at

locations just upstream and downstream of the test fixture and downstream of the primary heat exchanger. An Agilent ~~24570A~~ data logger was used to record measurements from the pressure transducer, thermocouples, and the heat sink RTDs. A Xantrex ~~programmable~~ programmable power supply controlled the power applied to the microchannel device heater. Both the data logger and power supply were configured and controlled over a GPIB interface with LabVIEW software.

RESULTS

The microchannel heat sink devices were tested for steady-state cooling performance. For a given flow rate and input heating power, the cooling loop was allowed to reach a state of thermal equilibrium as quantified by a temperature rise in the coolant of less than 2 °C/hr. Once reaching steady state, temperature and pressure data were collected at intervals of six seconds for approximately 30 minutes and then averaged. The coolant flow rate was monitored during this interval to insure a steady mass flow through the heat sink. Each test was performed at a loop system pressure of approximately 15 psig (200 kPa) with a coolant temperature of 21 °C at the inlet of the test fixture.

A test matrix comprised of flow rates from 10 to 25 ml/min and target cooling densities from 5 to 25 W/cm² was used to test the hydraulic and thermal performance of the microchannel heat sink devices. The voltage applied to the device heater was adjusted for each run so that the temperature rise in the coolant fluid across the test fixture would be equal to the desired cooling power divided by the product of the mass flow rate and coolant specific heat. This process allowed the data to be correlated based on heat flux into the microchannel heat sink device rather than total heater power consumption (which included parasitic heat losses from the test equipment.) Once the steady-state data was collected, the actual heat flux into the heat sink was determined from the net enthalpy change in the water and the mass flow rate.

Figure 5 shows the maximum chip temperature as measured by the platinum RTD located beneath the outlet manifold. From this plot, we can see that the silicon substrate was kept below the design limit of 80 °C for heat fluxes up to 23 W/cm². (A test with a heat flux greater than 25 W/cm² was not possible due to structural failure of the heat sink device.) Figure 6 also shows that higher chip temperatures are achieved at the same heat flux for lower flow rates, which is to be expected.

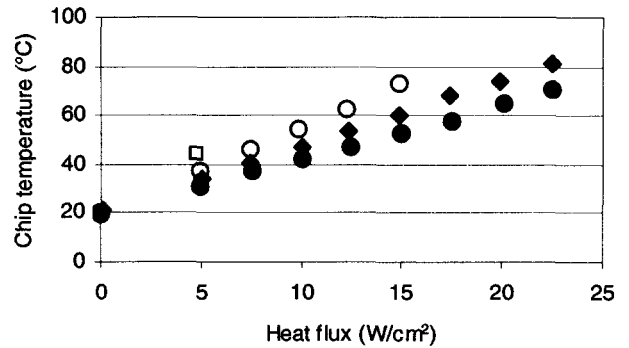


Figure. 5 Maximum chip temperature vs. heat flux for various coolant flow rates. Legend: ● 25 ml/min, ◆ 20 ml/min, ○ 15 ml/min, ◻ 10 ml/min.

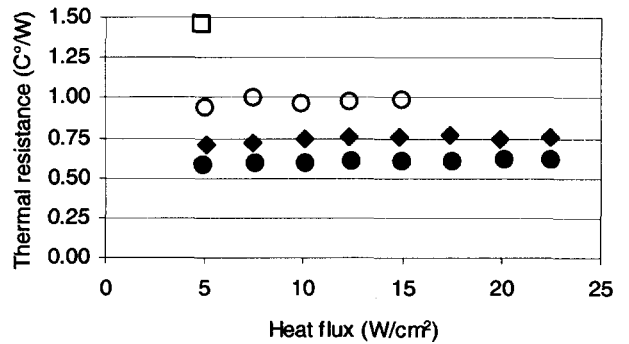


Figure. 6 Total thermal resistance vs. heat flux for various coolant flow rates. (see Fig. 5 for legend)

Figure 6 shows the variation of total thermal resistance of the heat sinks with heat flux and flow rate. Although there is little change in thermal resistance with heat flux, doubling the flow rate serves to approximately halve the resistance. This is largely due to the increased maximum chip temperature observed at the lower flow rates. Figure 7 shows the pressure drop across the devices for various flow rates and heat fluxes. It should be noted that the pressure drop through the test fixture is included in these data and serve to increase the pressure drop magnitude (albeit less than 10%). All pressure drops are below 0.5 psi (3.5 kPa)—well below the hydraulic performance design criterion of 2 psi. Additionally, there is a slight decrease in the pressure drop at the higher heat fluxes due to the decrease in the viscosity of the water as the temperature rises in the heat sink.